

AN IMPROVED GAAS MESFET MODEL FOR THE PULSED I-V MEASUREMENT

Kohei Fujii

Japan Radio Co., Ltd.
1-1 Shimorenjaku 5 Chome, Mitaka-Shi, Tokyo 181, Japan

Abstract

This paper describes an improved large signal model of the GaAs MESFET that agrees accurately with the I-V characteristics produced by the pulsed I-V measurement of the GaAs MESFET. The pulsed I-V measurement system developed and used to evaluate the performance of the model is also described. The calculated results for a microwave power amplifier predicted using an improved large signal model show good agreement with the experimental results obtained using the pulsed I-V measurement system.

Introduction

A number of GaAs MESFET equivalent circuit models [1-3] are available in commercial microwave circuit simulators. However, nonlinear CAD tool users and power MMIC amplifier designers are faced with inaccurate simulation results that are caused by the inaccuracy of the large signal model. To improve the accuracy of the results, the GaAs MESFET model should accurately model the following properties:

- 1) The drain conductance, G_{ds} , and the transconductance, G_m , are frequency dependent[4].
- 2) The saturation gain of the microwave MESFET is highly dependent on the breakdown characteristics[5].
- 3) The I-V curves of the GaAs MESFET are affected by the channel temperature[6].

The pulsed I-V measurement technique has been applauded for having advantage over the conventional static I-V measurement technique in large signal GaAs MESFET modeling. The pulsed I-V measurement results differ from the conventional static I-V

characteristics; however, there are no appropriate models for the pulsed I-V characteristics of the MESFET. Therefore, the improved model must be defined to agree accurately with the pulsed I-V characteristics of the GaAs MESFET. In this paper, an improved large signal model of the GaAs MESFET, which produces good agreement with the pulsed I-V measurement, is proposed. In addition, the pulsed I-V measurement system developed by the author is described.

Finally, an actual GaAs MESFET amplifier is described. Its performance is compared with the results predicted by simulation.

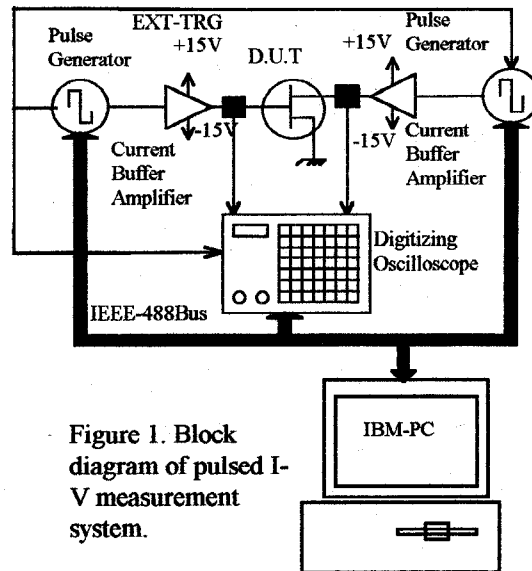


Figure 1. Block diagram of pulsed I-V measurement system.

Pulsed I-V Measurement

The block diagram of the pulsed I-V measurement system is shown in Figure 1. The pulsed I-V measurement system is capable of applying both positive and negative pulses that are superposed on the

operational d.c. bias voltages $((V_{br}-V_p)/2, Idss/2)$ in order to keep the best thermal agreement between measured and actual operation. A 1 μ sec pulse width and a 1kHz pulse repetition frequency were selected in order to realize the frequency dispersion of the output conductance and transconductance. To improve the current capabilities of the drain and gate pulse generators, current buffer amplifiers, which are commercially available high speed operational amplifiers, are used. The voltage and current capabilities of the drain and gate current buffer amplifiers are $\pm 13V$ and 1A, respectively. The gate and drain currents are sensed using inductive pick up probes, and the probe output signals corresponding to the drain and gate currents are displayed on a digital oscilloscope. All the test instruments have IEEE 488 bus capability. A desktop computer is used for control, data acquisition, and data processing.

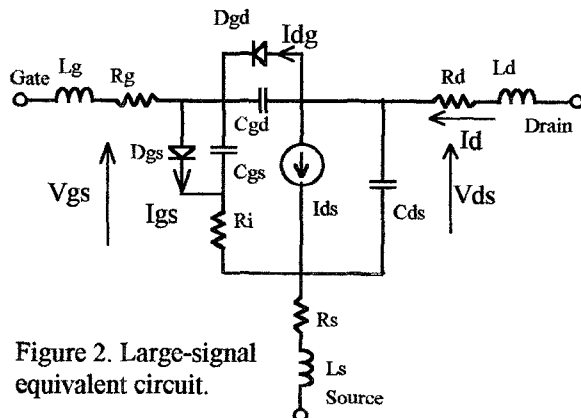


Figure 2. Large-signal equivalent circuit.

FET Model

In this work, a large signal model of the GaAs MESFET, which is improved to agree accurately with the pulsed I-V measurement results, has been developed. The new model can be represented by the equivalent circuit shown in Figure 2. In order to obtain an accurate agreement with the experimental pulsed I-V measurement results, a simple modification of the slope of the drain-source voltage in the well-known Materka model is proposed as follows.

$$I_{ds} = I_{dss} \left(1 - \frac{V_{gs}}{V_p} \right)^E \left(1 - \lambda V_{ds} \frac{V_{gs}}{V_p} \right) \quad (3)$$

$$\tanh \left(\frac{\alpha V_{ds}}{V_{gs} - V_p} \right)$$

$$V_p = V_{po} - \gamma V_{ds} \quad (4)$$

where $Idss$ is the saturation current (at $V_{gd} = 0V$), V_{po} is pinch-off voltage, and α, γ, E and λ are empirical constants. Each model parameter can be extracted using a global curve fitting technique between pulsed I-V measurement results and calculation results (eq.(1),(2)). The rest of the bias-dependent elements are the same as those used in the Materka model: the gate-source capacitance, C_{gs} , the gate-drain capacitance, C_{gd} , and the gate-source diode, D_{gs} . The parameters of the non-bias-dependent elements ($L_g, L_d, L_s, R_g, R_d, R_s, R_i, C_{ds}$) are extracted from the small signal S-parameter measurement results as well as the cold S-parameter measurement results[7].

Results

The drain current, Id , of a GaAs MESFET with 1200 μ m gate width and 0.5 μ m gate length was measured using both the pulsed I-V system and the conventional static system, and the results are shown in Figure 3. For the conventional static system, the IEEE-488 controlled power supply and multimeters were applied. Since the device is subject to physical degradation, a limited drain voltage sweep range was applied during the conventional static measurement. As shown in Figure 2, the drain current, Id , consists of two currents, the channel current, Ids , and the breakdown current, Idg . Figure 3 shows the difference between the pulsed I-V measured curve and the static I-V measured curve. The measured breakdown currents, Idg , are shown in Figure 4. This data shows that the proposed pulsed I-V measurement system can realize the device channel temperature effects, the frequency dependency of G_{ds} and G_m , and the device breakdown characteristics without any physical degradation.

The channel current, Ids , can be calculated from $Id - Idg$ shown in Figure 5. In Figure 5, the Materka model and the Fujii model are compared with the measured pulsed I-V results. All the model parameters were extracted using a global curve fitting technique. These results show that the accuracy of the Materka model is

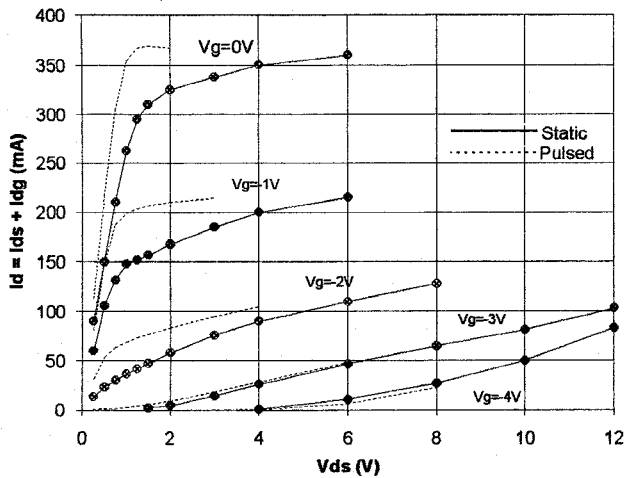


Figure 3. Comparison of pulsed and static I-V curve.

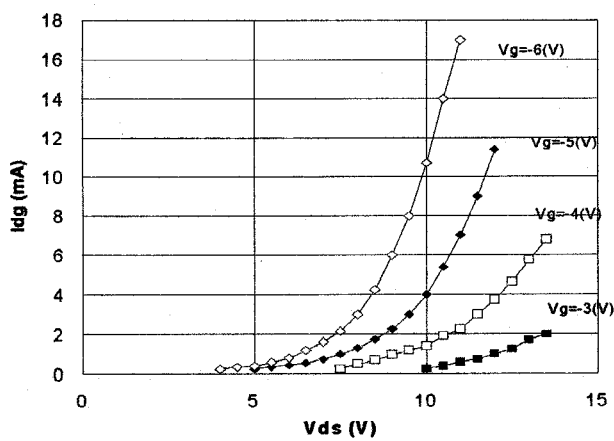


Figure 4. Breakdown pulsed gate current.

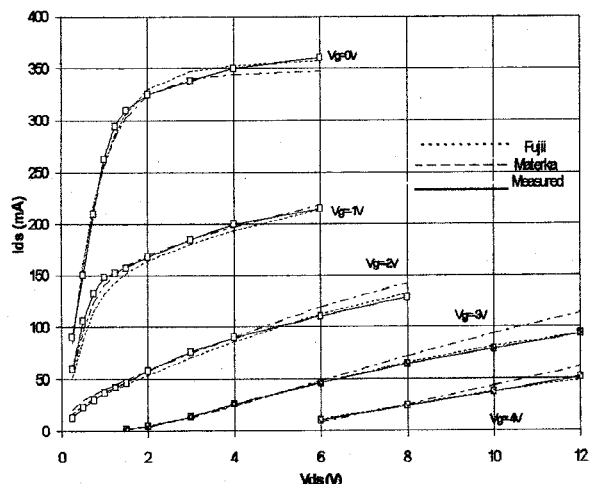


Figure 5. Comparison of measured and computed data.

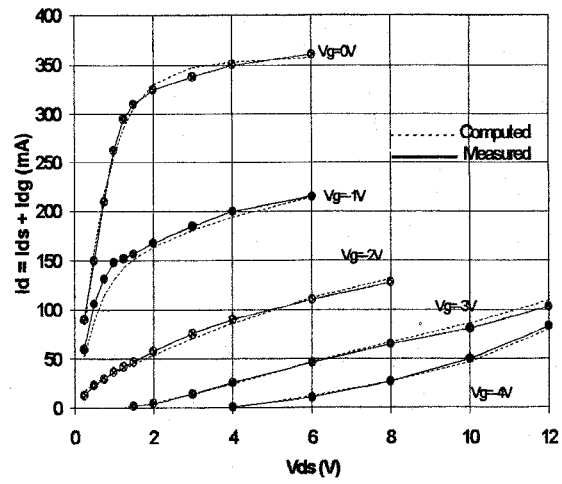


Figure 6. Comparison of measured and computed data for drain current.

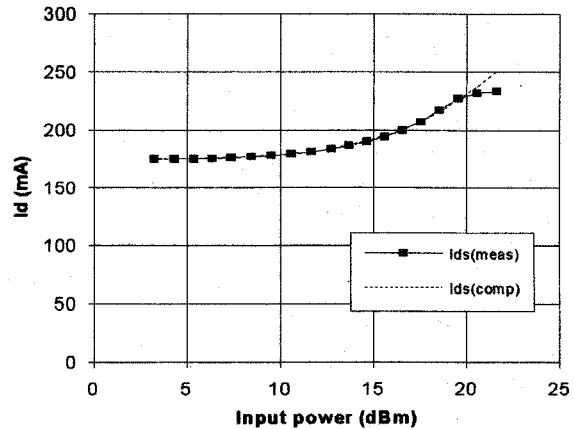


Figure 7. Measured and computed microwave power amplifier DC drain current performance.

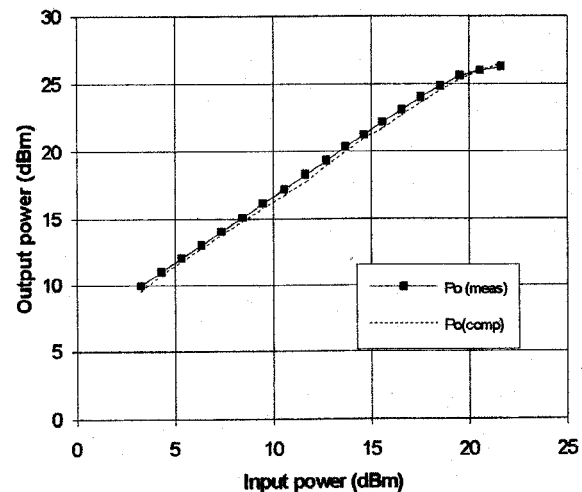


Figure 8. Measured and computed microwave amplifier output power performance.

somewhat poorer overall and deteriorates considerably as the drain current is reduced. On the other hand, the Fujii model offers real advantages in accuracy over the previous model. In the saturation region, the improved accuracy extends from high to low drain currents. This improved accuracy is the result of the inclusion of the λ parameter that improves the drain current slope versus the drain voltage, V_{ds} . The comparison between the measured drain current, I_d , including breakdown current, I_{dg} , and the computed currents is shown in Figure 6. As seen in Figure 6, the two data are very closely matched. Therefore, the Fujii model can be used to accurately simulate large signal microwave circuits.

Results of model verification for R.F. performance were given for the same power MESFET which had a $0.5\mu\text{m} \times 1200\mu\text{m}$ channel profile. A hybrid microwave amplifier was designed for narrow-band application at 10 GHz. The bias condition selected was the same as the pre-bias condition of the pulsed I-V measurement $((V_{br}-V_p)/2, I_{dss}/2)$. In this case, the power device was biased at $V_{ds} = 7$ V, $V_{gs} = -1.2$ V, and measurements were made at 10 GHz. Figure 7 and Figure 8 show the measured and simulated performance of input power vs. output power and drain current for a single-stage microwave power amplifier. The measured data was obtained using a spectrum analyzer and a signal source. The performance was simulated on the commercially available microwave non-linear simulator HP-MDS®. As is seen in Figure 7 and Figure 8, the pulsed I-V measurement and the improved I_{ds} model offer real advantages in predicting the performance of the large signal microwave power amplifier.

Conclusion

This paper has proposed an improved large signal model of the GaAs MESFET that agrees accurately with the pulsed I-V measurement curve. This model has been used to characterize a $1200\mu\text{m}$ MESFET. Excellent agreement between the measured results and the drain current data of the pulsed I-V model has been obtained.

The model has been used to study a microwave MESFET power amplifier. The output power saturation values and the drain current characteristics have been predicted and confirmed by experiments.

References

- [1] W.R. Curtice, "A MESFET model for use in the design of GaAs integrated circuits," *IEEE Trans. Microwave Theory and Techniques*, vol. MTT-28, pp.448-455, May 1980.
- [2] Y.Tajima, B.W.Worna and K.Misima, "GaAs FET large-signal model and its application to circuit designs," *IEEE Trans. Electron Devices*, vol. ED-28, pp.171-175, Feb.1981.
- [3] A. Materka and T.Kacprzak, "Computer calculation of large-signal GaAs FET amplifier characteristics," *IEEE Trans. Microwave Theory and Techniques*, vol. MTT-33, pp.129-135, Feb.1985.
- [4] J.Michael Golio, *Microwave MESFET's and HEMT's*. Boston: Artech House, 1991.
- [5] T.A.Winslow and R.J.Trew, "Principles of large-signal MESFET operation," *IEEE Trans. Microwave Theory and Techniques*, vol.42, No. 6, pp.935-942, June 1994.
- [6] A.Platzker, A.Palevsky, S.Nash, W.Struble and Y.Tajima, "Characterization of GaAs devices by a versatile pulsed I-V measurements system," *IEEE MTT-S Digest* pp.1137-1140, 1990.
- [7] E.Arnold, M.Golio, M.Miller, and B.Beckwith, "Direct extraction of GaAs MESFET intrinsic element and parasitic inductance values" *IEEE MTT-S Digest* pp.359-362, 1990.